SURFACE STRAIN MEASUREMENT FOR NON-INTRUSIVE INTERNAL PRESSURE EVALUATION OF A CANNON

BRENNAN LEE RAUSCH

Thesis submitted to the faculty of the Virginia Polytechnic Institute and State University in partial fulfillment of the requirements for the degree of

Master of Science
In
Mechanical Engineering

Wing F. Ng, Chair
Scott T. Huxtable
Robert L. West

August 4, 2022
Blacksburg, VA

Keywords: Gun System, Internal Pressure, Tangential Strain, Strain Gauge

SURFACE STRAIN MEASUREMENT FOR NON-INTRUSIVE INTERNAL PRESSURE EVALUATION OF A CANNON

BRENNAN LEE RAUSCH

ABSTRACT

The U.S. Army has recently developed cutting edge designs for gun barrels, projectiles, and propellants that require testing. This includes measuring the internal pressure during fire. There are concerns with the current method of drilling to mount pressure transducers near the breech and chamber of the gun barrel where pressure is highest. An alternative, non-intrusive strain measurement method is introduced and discussed in the present work. This focuses on determining the feasibility and accuracy of relating tangential strain along the sidewall of a gun barrel to the drastic internal pressure rise created during combustion.

A transient structural, numerical modal was created using ANSYS of a 155 mm gun barrel. The pressure gradient was derived using a method outline in IBHVG2 (Interior Ballistics of High Velocity Guns, version 2), and the model was validated using published experimental tangential strain testing data from a gun of the same caliber. The model was used to demonstrate the ideal location for strain measurement along the sidewall of the chamber. Furthermore, three different pressure ranges were simulated in the model. The behavior of the tangential strain in each case indicates a similar trend to the internal pressure rise and has oscillation due to a dominant frequency of the barrel. A method to predict internal pressure from external tangential strain was developed. The internal pressure predicted is within 4% of the pressure applied in the model. A sensitivity study was performed to determine the primary factors affecting tangential strain. The study specifically looked at material properties and geometry of the gun barrel. The thickness and elastic modulus of the gun barrel were determined the most relevant. Overall, the present work helps to understand tangential strain behavior on the sidewall of a large caliber gun barrel and provides preliminary work to establish an accurate prediction of internal pressure from external tangential strain.

- SURFACE STRAIN MEASUREMENT FOR NON-INTRUSIVE INTERNAL PRESSURE EVALUATION OF A CANNON

BRENNAN LEE RAUSCH

GENERAL AUDIENCE ABSTRACT

Innovative technology for large gun systems require testing to evaluate safety and performance. The most recent designs from the U.S. Army for long range artillery require higher pressures. Currently, large gun barrels are drilled to mount pressure transducers for internal pressure testing, but the new generation of weapons require a way to measure internal pressure of the gun without introducing these high stress locations. External strain offers a means to measure displacement of the barrel caused by the internal pressure change with minimal alteration to the gun barrel.

The present work focuses on modelling a large gun barrel using finite elements to understand the behavior of strain on the external surface due to internal pressure during fire. Measurements were taken near the chamber of the gun barrel model. The strain behavior is comprised of two components, a linear change due to a pressure increase and vibrations introduced due to the sharp pressure increase over a short amount of time. Three cases were evaluated at different pressure ranges and a method was developed to predict internal pressure from the tangential strain with a maximum error of 4% for all cases studied. The model also indicates that the strain results are most sensitive to a change in thickness and the elastic modulus of the gun barrel material.

Acknowledgements

First, I would like to thank my advisor, Dr. Ng, for all his advice and encouragement. This work would also not be possible without Dr. Hang Ruan, Dr. Echo Kang, and Mr. Albrey de Clerk of NanoSonic Inc and my research team members: Scott Mouring, Jason Stiefvator, and Patrick Cole. Thank you all for your support. I also would like to acknowledge and thank my committee members for their advice and invaluable knowledge. Finally, I would like to thank my friends and family for their unwavering love and motivation throughout this process.

Contents

List of Figures

List of Tables

SURFACE STRAIN MEASUREMENT FOR NON-INTRUSIVE INTERNAL PRESSURE EVALUATION OF A CANNON

1 Introduction

Internal pressure of gun systems reveals characteristics about the performance, safety of the barrel, as well as the type of ammunition or projectile used. Commercial manufactures follow SAAMI (Sporting Arms and Ammunition Manufacturers' Institute) standards for internal pressure measurements during fire that require mounted pressure transducers [1]. Small arms users can follow these manufacturer's guidelines and technical data sheets for approximate barrel pressure. For large caliber cannons used by the Army, these pressure transducers are mounted along the gun barrel like small caliber guns. The sensors measure various characteristics such as the maximum loading in barrels, comparing pressure- time (P-T) curves for different projectile types, and comparing P-T curves at distinct locations along the gun barrel [2].

Moving forward, a large caliber gun system used by the Army is discussed. For the specific application studied, transducers are normally mounted near the breech of the gun, while another is mounted along the chamber, referenced in

Figure 1. The difference in pressure at these locations can cause structural damage to the breech under the right conditions and the difference can be minor compared to the maximum pressure experienced. Due to this, pressure measurements are vital to testing large gun systems; however, transducers are becoming a limiting factor in recent design. When testing recent technology for long range artillery, specifically, advanced cannons, projectiles, and propellants, the accuracy of the pressure measurement is extremely important when there is no historical data. There are also safety concerns that long range artillery designs cause higher stress in the barrel than previous versions. Due to the current method of drilling to mount these sensors and introducing potential failure points along the barrel, testing cannot move forward. To further the issue, depending on the projectile and propellant type tested, additional locations may be needed to measure pressure. To assess this new technology, a non-intrusive method must be created to accurately measure internal pressure and hold the same standards and accuracy as previous tests.

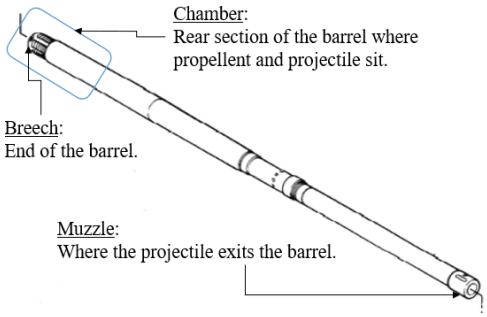

Figure 1: Gun Barrel Section Terminology

Non-intrusive, strain measurement is proposed in the work as an alternative testing method. Once there is an internal pressure rise in the gun barrel from combustion of the propellant, this will induce strain within the walls of the barrel. The relationship between internal pressure and external strain, like in high-pressure vessels, is well documented and expressed using the theory of elasticity [3]. Focusing on the outside of a gun barrel, or more simply, a cylinder, the strain is introduced in three principal directions: longitudinal, radial, and tangential as shown in Figure 2. The radial strain is inconsequential, as pressure reaches atmospheric on the surface. Additionally, the tangential strain is greater than the longitudinal strain due to geometry. Therefore, the tangential strain, also referred to as the tangential or circumferential strain, provides the best direction for measurement. The theoretical relationship between static internal pressure (P_i) and tangential strain (ε_t) is written in Eq. 1 [3]. Nomenclature is in Appendix A. However, firing a gun which happens within milliseconds introduces other transient conditions. Specifically, the sharp pressure rises causes vibration in the gun barrel. Water hammer studies, producing a similar environment with a moving pressure shock inside a cylinder discuss this vibration in detail. The work of Leishear describes the oscillation introduced in a cylinder at an exact location from a step pressure change [4]. This can be thought of as 'breathing'; the cylinder walls expand and contract.

$$\varepsilon_t = \frac{r_i^2\, P_i}{r_o^2 - r_i^2} \cdot \left(1 + \frac{r_o^2}{r^2}\right) \cdot \left(1 - \frac{\nu}{2}\right) \cdot \frac{1}{E} \qquad (1)$$

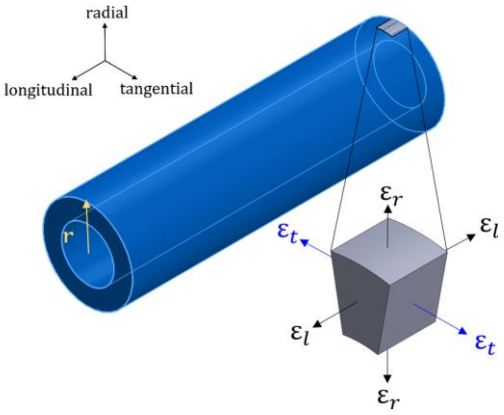

Figure 2: Strain on the Outside of a Cylinder

Strain gauge sensors provide the means to measure strain when mounted in the tangential direction. There are notable benefits using these over a pressure transducer as well. The most relevant is mounting these sensors require minimal alteration to the surface. Stain gauges are also manufactured usually in small, discrete packaging and offer location

flexibility. Recent strain gauges designed by NanoSonic Inc., demonstrate sensors high sensitivity to strain (on the micro-strain level) and large frequency range (up to MHz) [5]

In literature, the dynamic tangential strain of gun barrels has previously been measured experimentally as well as using finite element models. Dynamic strain amplification or the increase in maximum strain compared to strain under static inputs was modeled in a large caliber gun. Hopkins used the model to study the increase in tangential strain amplification due to projectile velocities and compared the model results to theoretical calculations [6]. Tangential strain has also been used to validate a 40 mm gun barrel model however the error or difference between the experimental and model results was not quantified [7]. Additionally, an experiment for a 155 mm gun barrel used strain gauges to approximate the internal pressure near the muzzle, but only compared this to theoretical internal pressure calculations [8]. Although, there has been advancement using this strain method for pressure measurement in smaller systems. The Pressure Trace II is an at home hardware and software package utilizing a strain gauge to predict internal pressure for rifles. The main drawbacks for this system are firstly the limited pressure range for quality resolution and secondly the static pressure assumption for calculations [9]. Overall, the strain method proposed to measure internal pressure for large gun systems has not been directly studied before.

Due to the limited work on using strain gauges for internal pressure measurement of large guns, the goal of this project is to show the feasibility of using tangential strain to accurately predict internal pressure. This study includes an initial numerical analysis to predict tangential strain results for a 155 mm gun barrel with a full understanding of strain behavior and provides initial conclusions about the relationship between external tangential strain and internal pressure measured on the sidewall of a finite element gun barrel model under transient conditions.

2 Governing Physics

This section provides an overview of the governing physics of the gun system's internal pressure. This will be used to predict pressure behavior at unknown locations on the gun barrel and generate P-T curves to input into a finite element model. A brief description of the calculation for the pressure gradient or pressure in space and time, P(x,t), inside the barrel is provided along with relevant assumptions.

The pressure gradient inside the gun barrel is predicted using the derivation method from the Interior Ballistics of High Velocity Guns, Version 2 (IBHVG2), a theoretical calculation, and uses experimental pressure data to calibrate the equation [10].

2.1 Pressure Gradient Derivation

The gaseous propellant between the breech ($x = 0$) and projectile base ($x = x_p$) seen in Figure 3 can be described using Euler's equations of continuity and momentum in Eq. 2 and 3. The projectile at x_p moves down the barrel with respect to time. Also note that the breech is considered fixed, as recoil has a small effect on pressure predicted, and assumed inconsequential in these calculations [11].

$$0 = \frac{\partial \rho}{\partial t} + \frac{\partial}{\partial x}(\rho v) \quad for\ 0 \le x \le x_p \tag{2}$$

$$\frac{-1}{\rho}\frac{\partial P}{\partial x} = \frac{\partial v}{\partial t} + v\frac{\partial v}{\partial x}\ for\ 0 \le x \le x_p \tag{3}$$

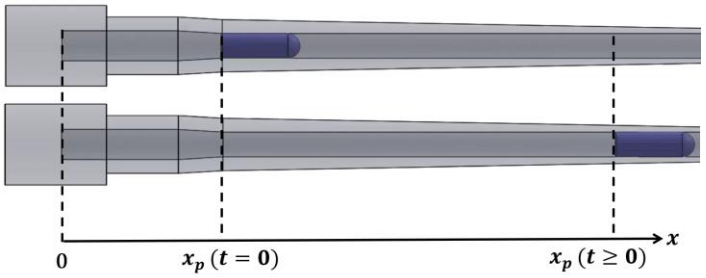

Figure 3: The Projectile Moving Boundary Over Time

The propellant is treated as completely gaseous and uniformly distributed spatially at every point in time, so $\frac{\partial \rho}{\partial x} = 0$ in Eq. 2. Additionally, the velocity of the gas is described as zero at the breech, $v(0,t) = 0$, and equal to the projectile velocity at the base, $v(x_p,t) = \dot{x}_p$. Under these boundary conditions and assumptions, the gas velocity can be written in terms of the projectile motion: $v = x\frac{\dot{x}_p}{x_p}$. Additionally, since the propellant is treated as uniformly distributed, the density is described as the propellant mass (C) divided by the volume from breech to base where A_p is the cross-sectional area of the projectile. Therefore, Eq. 3 can be rewritten.

$$P' = -\rho\frac{x}{x_p}\ddot{x}_p = -\left(\frac{C}{A_p x_p}\right)\left(\frac{x}{x_p}\right)\ddot{x}_p \tag{4}$$

Moreover, the acceleration of the projectile is rewritten using Newton's Second Law. This includes frictional forces and air resistance acting against the direction of motion seen in Figure 4. Thus, the pressure gradient is written using these terms.

$$P' = -\left(\frac{C}{A_p x_p}\right)\left(\frac{x}{x_p}\right)\frac{A_p(P_{base} - P_{res} - P_{air})}{m_p} \tag{5}$$

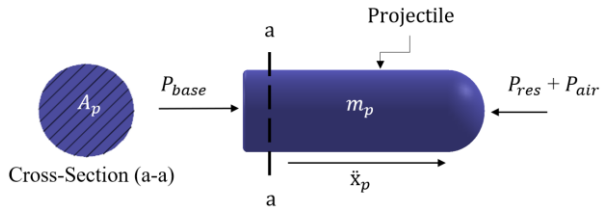

Figure 4: Projectile Free Body Diagram (FBD)

Integrating from breech to base, the final equation is given as

$$P(x,t) = P_b - \frac{C(P_{base} - P_{res} - P_{air})}{2m_p}\frac{x^2}{x_p^2} \qquad (6)$$

where $P(0,t) = P_b$ and $P(x_p,t) = P_{base}$. Therefore, to fully describe the pressure inside the barrel, this method requires knowledge of the projectile location (x_p), mass (m_p), and forces (P_{base}, P_{res}, P_{air}) as well as the propellant mass (C) and breech pressure ($P_b = P(0)$).

The pressure transducer locations on a currently operating gun barrel are shown in Figure 5. The Army's Yuma Proving Ground (YPG) has provided breech pressure and sidewall pressure ($P_s = P(x_s)$) of a 39-cal, 155 mm gun barrel for three different firing tests. One example pair of pressure curves is shown in Figure 6. The point in time when the projectile exits the barrel is designated at $t = 0$.

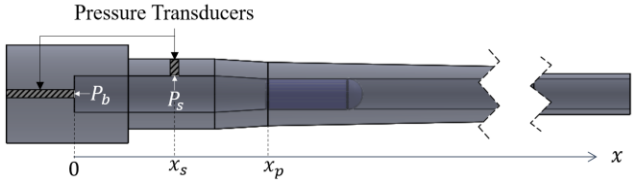

Figure 5: Pressure Transducer Locations

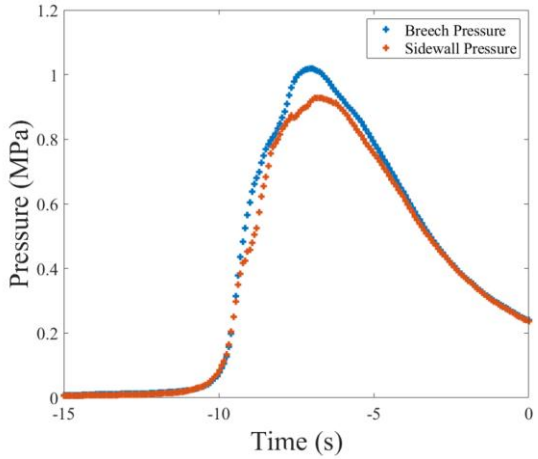

Figure 6: Pressure vs. Time Data

Both curves are used to determine the unknown constants in Eq. 6. The breech pressure is substituted in the first term as a boundary condition while the sidewall pressure is used to match unknown values in the second term. These unknown variables are designated feasible ranges. For example, Army literature indicates the projectile mass should be within 30 to 40 kg. Next, a random selection is made within these ranges, and the pressure gradient is calculated. An iterative process is used until YPG's sidewall pressure matches well with Eq. 6 when $x = x_s$. This comparison is described in more detail in Appendix B, giving the optimal values for each of the three shots provided by YPG. The final $P(x_s, t)$ compared to YPG's sidewall pressure is also plotted in Appendix B for each case.

3 Model Setup

To model a large caliber gun system during fire, some assumptions are made to simplify the gun barrel while maintaining a well-posed model. After multiple rounds there is normally a temperature increase in the barrel and a potential for thermal expansion causing residual stress. However, in this study, the model is at a uniform, stress-free temperature on the outer surface when assuming a single round is fired [12]. The projectile-barrel interaction is not incorporated since the chamber area where the pressure is normally measured does not interact with the moving projectile. Additionally, residual stresses introduced in the manufacturing process due to autofrettage of the gun barrel are not incorporated at this time since the plastic range zone of the barrel material is closer to the inner surface [13] and beyond the scope of this project.

3.1 Geometry

Considering the gun barrel symmetry and isotropic materials, the gun barrel is treated as an axisymmetric, single part. The length and caliber are based on a 39-cal, 155 mm gun barrel and shown in Figure 7 with relevant dimensions listed in Table 1. Note that the barrel narrows and the outer radius is reduced along the length of the barrel [14]. The outer radius of a large gun barrel measured is used to establish the minimum thickness that can be used in the model.

Table 1: Important Geometry of Gun Barrel Model

Geometry	Value
Gun Barrel Length, L	6.045 m
Inner Radius, IR	93 mm (before narrowing) 77.5 mm (after narrowing)
Outer Radius, OR	164 mm → 99 mm

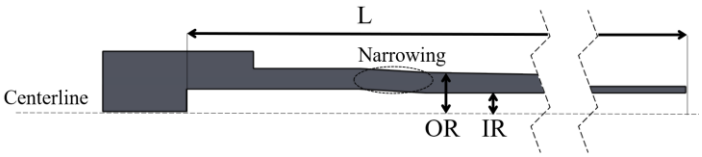

Figure 7: Axisymmetric Gun Barrel Model

3.2 Material Properties

The gun barrel material properties are summarized in Table 2 and based on the Army Research Laboratory (ARL) M256 cannon material [6]. This reflects the properties of a high strength steel alloy and are homogeneous throughout the model.

Table 2: Model Gun Barrel Material Properties

Material Property	Value
Elastic Modulus, E	200 GPa
Poisson's Ratio, ν	0.30
Density, ρ	7700 kg/m^3

3.3 Initial and Boundary Conditions

The model has a fixed near the breech, so displacement and centerline rotation are set to zero. The pressure boundary

condition is specified to load the internal edge of the gun barrel model using pressure versus time (P-T) curves. The barrel is sectioned along its length (seen in Figure 8) so that the pressure versus time is calculated at a section location and the resulting P-T curve is applied to the internal edge of that section. Note that these P-T curves are calculated from the pressure gradient equation at specific locations to simulate a moving pressure wave down the barrel. Examples of the P-T curves shown in Figure 9. Refer to Figure 8 for an illustration of the boundary conditions. An independence study was performed to determine the necessary spatial sections (400) in the model to represent the pressure gradient. This is shown in Appendix C.

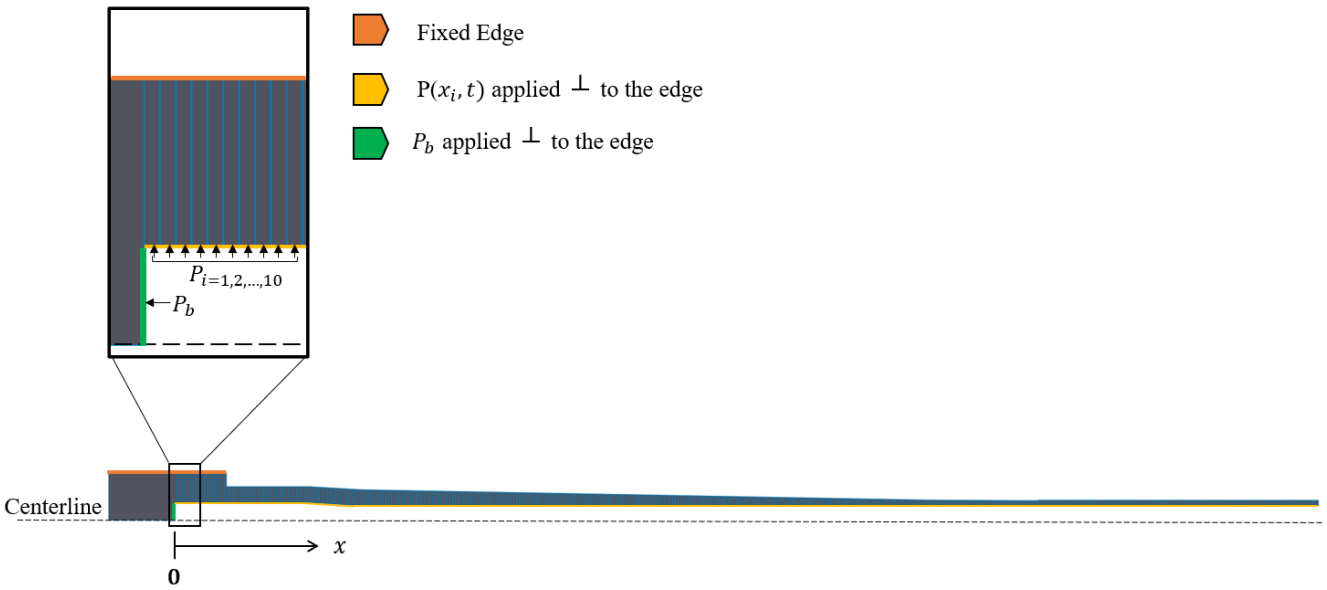

Figure 8: Boundary Conditions of the Gun Barrel Model

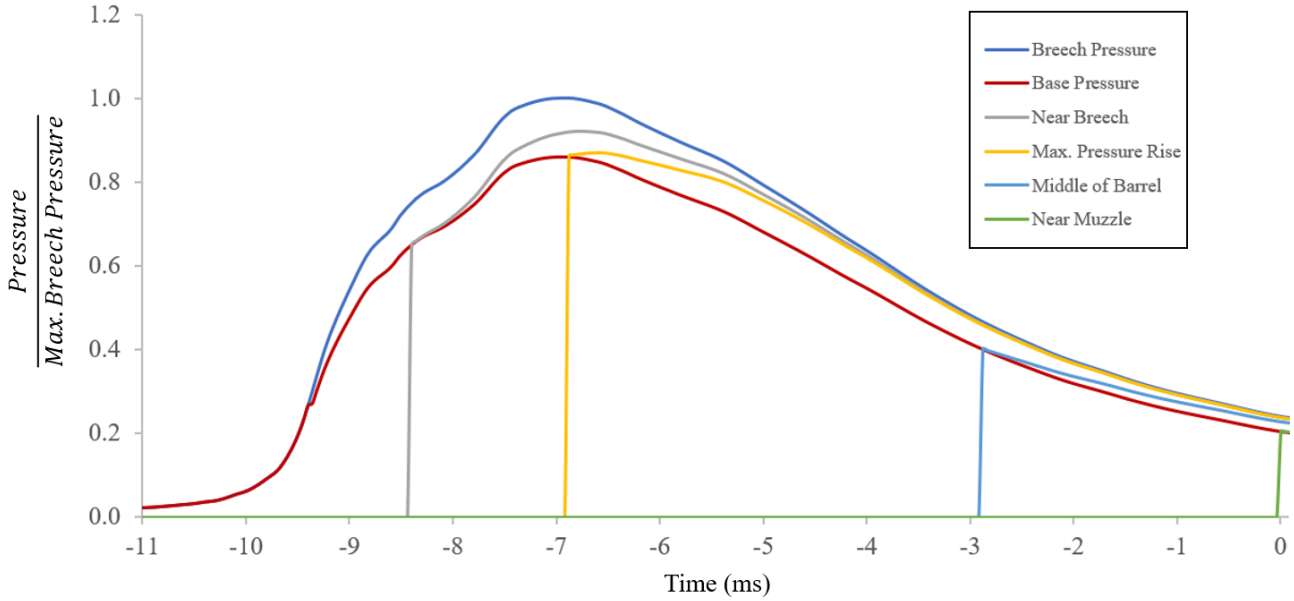

Figure 9: Input Pressure vs. Time Curve Examples

3.4 Damping

Viscous damping is included using the Rayleigh Damping method. It uses a linear combination of the mass and stiffness matrices where the alpha and beta are the respective coefficients to the mass and stiffness terms. This is used to designate a damping ratio at the dominant frequencies found using modal analysis of the gun barrel. In this case, the frequency range is between 5 kHz to 10 kHz. Since there is little to no information on the damping ratio of the system, it is calibrated and set to 0.003. This calibration of the damping ratio is discussed later. Appendix D goes into detail to select the frequency ranges and calculating the Rayleigh coefficients.

3.5 Mesh

The gun barrel is meshed using a single quadratic, axisymmetric element type, PLANE 183, for the entire barrel seen in Figure 10. This element type allows two displacement degrees of freedom and provides quadratic displacement interpolation. Sections of the barrel have consistent element sizing with nodal matching between each. A grid independence study was performed. The model is set up using the boundary conditions described previously. Therefore, a pressure gradient is applied to the internal edges of the gun barrel model. Then, the maximum strain measured at an external edge is taken (ε_{coarse}). The model's mesh is then refined, the model is run again, and maximum strain is measured again at the same location (ε_{fine}). This process is repeated until the maximum strain measure is consistent with previous results. and the global element size (6mm) is set so every section has at least two elements across with a 1:1 aspect ratio.

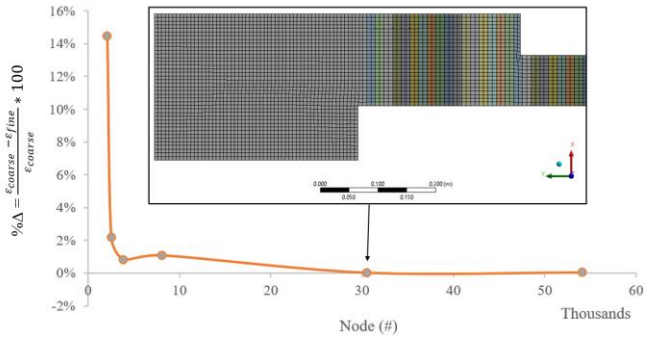

Figure 10: Grid Independence Study

3.6 Solution Method and Verification

The model is solved using the Transient Structural Solution method in ANSYS 2020 R2. Time stepping is used at 25 kHz – 200 kHz frequency and set to automatically use necessary sub steps for time increments where there is a large step in pressure. An 18 core, Intel Xeon W-2295 3.0 GHz workstation with 64 GB of RAM was used to solve the system of equations.

To verify the model setup, an analytical analysis of tangential strain due to static internal pressure was first conducted. Then, a transient analytical analysis was used to compare the vibration results of an internal step pressure change. A response frequency was derived using energy conservation and vibration of a SDOF oscillator [4]. The analytical solution and numerical model are in good agreement, giving confidence in the solution method. More details on verifying the numerical solution are contained in Appendix E.

4 Model Validation

The model geometry, material properties, and pressure gradient are all approximated based on general knowledge of a large caliber gun system and information provided by YPG. Due to this, the model requires some comparison to experimental data to validate the model. Therefore, the tangential strain model results are compared to published experimental strain data of a 155 mm gun system at a maximum breech pressure close to 360 MPa [8]. The testing setup from this paper is briefly described, and a strain results comparison is made.

This experiment was used to study barrel-projectile interaction and therefore sensors were placed downwind of the breech. Specifically, strain gauge sensors are mounted in the tangential directions at four locations (S1, S2, S3, S4) in 0.5 m increments from the muzzle [8], as shown in Figure 11. Only cases where breech pressure reaches close to 360 MPa are used for comparison. At a breech pressure of this magnitude, the driving band on the projectile, used for normal contact to internal walls of the gun barrel, is significantly worn. If this driving band is not worn down, significant jumps in strain occur due to the normal force of the driving band. Since the projectile is not incorporated into this model, higher charges are used for comparison.

The pressure gradient in the model is calculated using Eq. 6 and calibrated using zone 5H (close to 360 MPa maximum breech pressure). The pressure experienced at the sensor locations, the time it takes the projectile to exit (shot-out time), and the muzzle projectile velocity stated in the experiment match well with the corresponding values predicted in the ANSYS model. Before the experiment described above, the study uses internal ballistic calculations to predict the maximum pressure at the sensor locations along the barrel [8]. The pressure gradient at the same locations is slightly raised to better match the maximum pressure rise (within 3 – 7%). The shot-out time matches within less than 1 ms of the model conditions. Finally, the projectile velocity at exit is approximately 863 m/s while the model's simulated pressure wave reaches the exit at 867 m/s.

Figure 11: Experiment's Strain Gauge Locations Along the Gun Barrel

4.1 Comparison to Tangential Strain Experimental Data

It should be noted that the initial tangential strain results of the model did not match experimental data due to damping. The damping is unknown for this gun barrel and the value is adjusted to have a better calibrated model. The damping ratio (0.003) is selected to best match the amplitude of oscillation. The amplitude of oscillation before the pressure increase is compared where experimental results and model results are 65 – 75 με and 60 -90 με respectively. However, the amplitude is overpredicted in all locations after the pressure wave passes where experimental results are 16 - 24 με. The final comparison is shown in Figure 12.

Overall, the maximum tangential strain measured at each sensor location is within 2% agreement to the model results

except at S2. The experimental data at S2 show consistently higher tangential strain in time, about a 7% difference. This is still within reasonable error, as the predicted internal pressure in the experiment and model's pressure gradient were not exactly equal. The pressure gradient used in the model predicts that internal pressure at t = 0 (shot-out time) is consistent at all locations within the gun barrel, indicating that the tangential strain should be consistent if all else is the same. Therefore, the significant difference in tangential strain at S1at t=0 is due to the larger thickness at this location. The thickness between S2, S3, and S4 changes no more than 1 mm which follows that the tangential strain near t = 0 is similar. Another distinguishing feature seen in the transient results is the oscillation. Experimental data show a response frequency between 7 – 9 kHz, while the model results predict between 6 – 10 kHz. The amplitude of oscillation matches well with before the pressure increases. However, is slightly overpredicted after passing. The velocity matches well, measured using the drastic strain increase at each location.

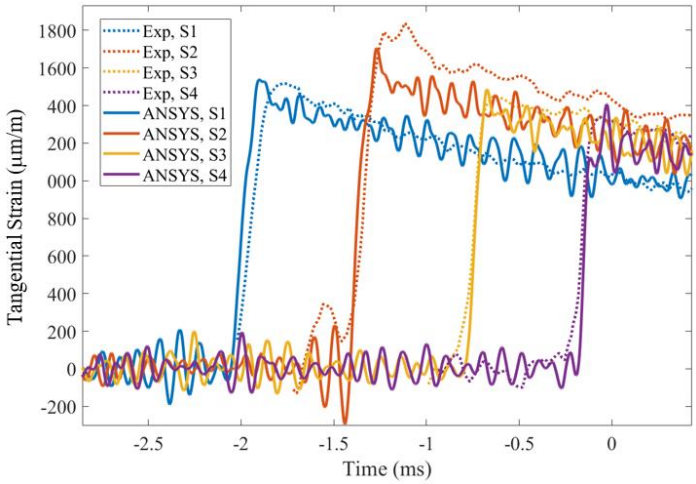

Figure 12: Tangential Strain Comparison of Model and Experimental Data

5 Results and Discussion

Once the model was developed and validated using experimental strain data, it was used to extrapolate results and perform a design study. Before this, a location near the breech is selected to provide the maximum measurable tangential strain. This matches well with the current location of pressure transducers. Then, the three cases provided by YPG (5H, 4H, and 3H zones) were modeled to study the strain response. Specifically, the maximum strain and frequency response are discussed and a relationship between tangential strain and internal pressure is approximated. A design study was performed to distinguish the primary factors that tangential strain is the most sensitive to.

5.1 Location Selection

The optimal place for strain measurement is defined here as the location where the largest tangential strain can be measured. In this model, the thickness and maximum internal pressure experience (base pressure) are primary factors. The base pressure of zone 5H and measurable tangential strain are plotted along the length of the gun in Figure 13**.** Note that the thickness of the gun barrel decreases along the length, driving the measurable tangential strain up, especially within the first meter. Also, the applied maximum pressure near the chamber is significantly larger than the rest of the gun barrel, so the optimal location of measurement is at x = 0.48 m. Note that near the end of the muzzle near 4.0 – 4.5 m, the tangential strain shows a local maximum as the thickness reduces rapidly and could be a potential location of interest as well. If the barrel's thickness is slightly reduced or pressure applied in this area is relatively larger for other cases, this could also be considered an optimal location.

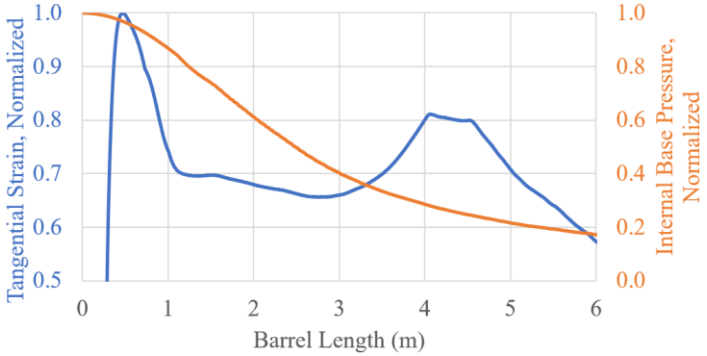

Figure 13: Base Pressure and Tangential Strain vs. Barrel Length

5.2 Extrapolating Strain Results

Once the model has been validated and an ideal strain measurement location is selected, the model is used to extrapolate strain results at x = 0.48 m for three different propellant amounts. The breech pressures and sidewall pressures provided by YPG for each case are shown in Figure 14. They are referred to as zones 5H, 4H, and 3H. The amount of propellant used decreases for each, respectively. This in turn decreases the overall velocity and internal pressure at descending zones. Thus, the maximum pressures are 360 MPa, 225 MPa, and 135 MPa, respectively. The pressure gradient for each is calculated in Appendix B.

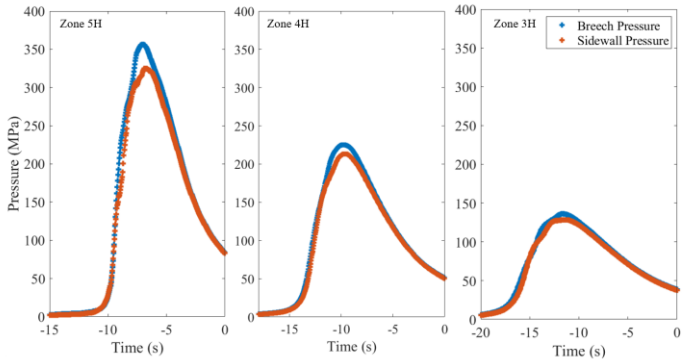

Figure 14: Breech & Sidewall Pressure for Zones 5H, 4H, and 3H

The results for these three cases predicted behavior similar to the pressure input at the measured location with a

dominating frequency, as previously seen in the experimental results section. The dominant frequency for each is at 6.844 kHz. The predicted internal pressure is based on two components. One is the linear relationship between tangential strain and internal pressure under static conditions shown in Eq.1. The difference (13.4%) between the model and predicted results due to geometry are discussed in Appendix E is also considered. Secondly, the vibration of the gun barrel is considered. To relate the tangential strain results to the internal pressure, a lowpass IIR (infinite impulse response) filter set to 1 kHz is first applied. This eliminates the vibratory signal at 6.844 kHz and maintains the working signal occurring over a 12 to 20 ms time span. Then, the filtered data is inserted into Eq. 1 to solve for internal pressure. The final step is to multiply by a correction constant due to the 13.4% difference. A comparison of predicted internal pressure and actual pressure applied in the model for all cases is seen in Figure 15. There is an initial large error (50%) lasting less than 0.5 ms for each case. However, the rest of the time, the error stay within ± 4% in all cases. At the largest pressure for each case this could be ± 13 MPa, ± 8MPa, and ± 5MPa for zones in 5H,4H, and 3H respectively. The actual pressure in all cases is overpredicted as the pressure rises and underpredicted just before maximum pressure is reached and thereafter. This may indicate a phase shift between the predicted and actual pressure experienced caused by the type of filter used. Each case shown in Figure 15 highlights that the pressure is very closely predicted and is a key finding for this simple model.

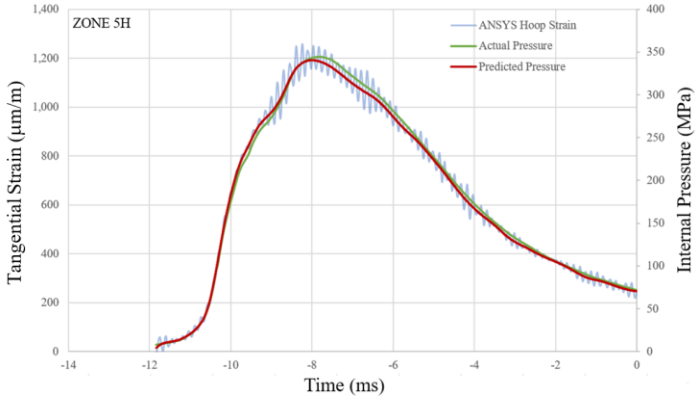

(a) Zone 5H

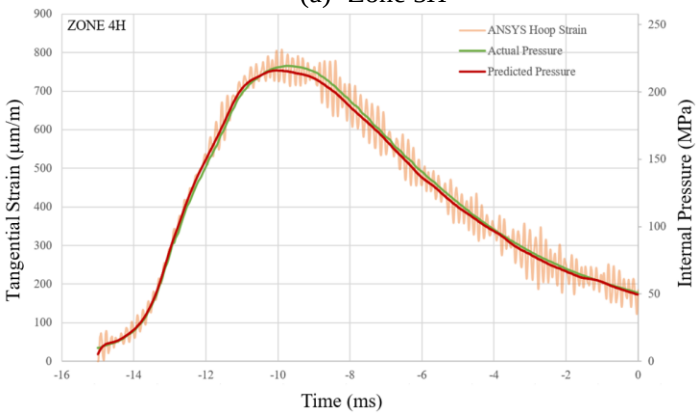

(b) Zone 4H

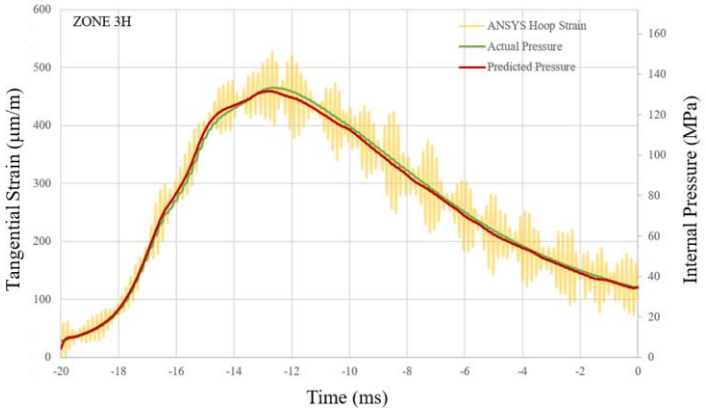

(c) Zone 3H

Figure 15: Predicted and Actual Internal Pressure Results

5.3 Sensitivity Study

Different parameters of the gun barrel are studied to determine the effect they have on tangential strain response. Specifically, the geometry and material properties are varied, while the maximum tangential strain and frequency response using the FFR (Fast Fourier Transform) method are predicted. Understanding the sensitivity of tangential strain to these variables should give insight to model the gun barrel more accurately and understand the effect of slight variations within large caliber gun systems. The primary parameters contributing to a change in tangential strain response are identified.

The gun barrel is studied using four parameters, the thickness of the barrel, elastic modulus, poison's ratio, and density. Each parameter is altered individually to make sure results are independent. Since the thickness changes throughout the length in the original model described previously, for this study, the outer radius is kept consistent for each case along the length; The first case is set to 180 mm for the outer radius and following cases are increased to 220 mm. For material properties, the elastic modulus is varied between 180 GPa to 210 GPa. Poisson's Ratio is varied between 0.26 and 0.30, and the density is increased from 7700 kg/m^3 to 8100 kg/m^3. These material property ranges are selected to be within reasonable consideration for high strength steel alloys. The baseline model for this study has no viscous damping and percentages are given with reference to the smallest values within each range (Ex. 180 mm – 220 mm with 180 mm as reference).

5.3.1 Primary Parameters

The tangential strain results are taken at the sidewall location along the chamber discussed previously (x = 0.48 m). The thickness and elastic modulus resulted in the largest changes as seen in the tangential strain results in Figure 16 and Figure 17 respectively. The tangential strain results due to change in thickness from 180 mm to 220 mm are shown in Figure 15 and indicate a significant reduction in tangential strain. The maximum strain decreased 42% across the total range. This lines up very closely with expected strain assuming static conditions. Similarly, the amplitude of oscillation also

reduces approximately 81%. This is crucial as the maximum strain measured at 180 mm thickness is becoming relatively high compared to the overall magnitude. Out of all parameters studied, the thickness was the only factor that had a consequential effect on the dynamic strain amplitude. This is largely attributed to the exponentially increasing mass in the location. The dominant frequency also seemed to shift downwards about 6% with increasing thickness. The elastic modulus also caused notable changes in the tangential strain. As the elastic modulus increased in value, the maximum strain predicted decreased 10% across the entire range. As the elastic modulus becomes larger, the dominant frequency increases about 5%. In Figure 17, a section of the results is enlarged to clearly see the dominant frequency shift.

5.3.2 Secondary Parameters

Other parameters, the density and poison's ratio, showed minimal change in the frequency without any obvious differences. Figure 18 shows the resulting change shift in dominant frequency as density increases. The frequency response reduces about 1% across the entire range. A change in Poisson's Ratio acts in the same manner across the 0.26 to 0.30 range (frequency decreases as Poisson's Ratio increases).

From these results, it is imperative to accurately model the thickness as well as elastic modulus of the gun barrel. The dynamic amplitude is especially sensitive to a change in thickness which is common in large gun systems. Additionally, the dominant frequency is not particularly sensitive to any of the four parameters. The design study is summarized in Table 3.

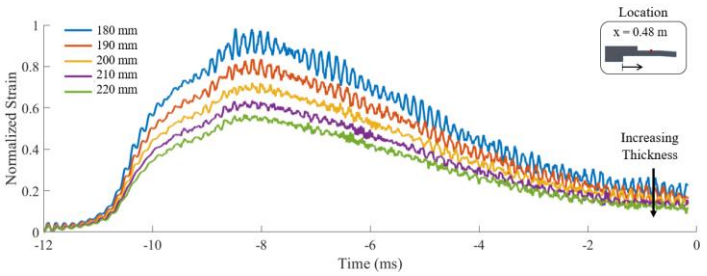

Figure 16: Normalized Tangential Strain Results for Changing Thickness

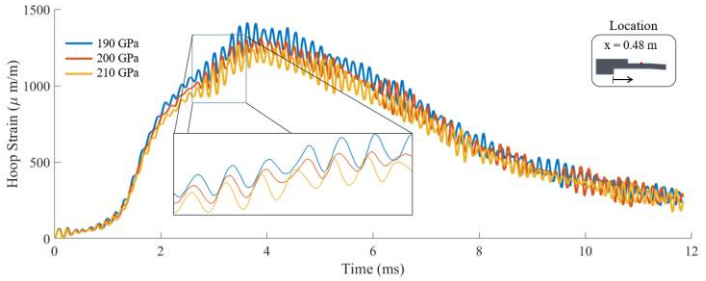

Figure 17: Normalized Tangential Strain Results for Changing Elastic Modulus

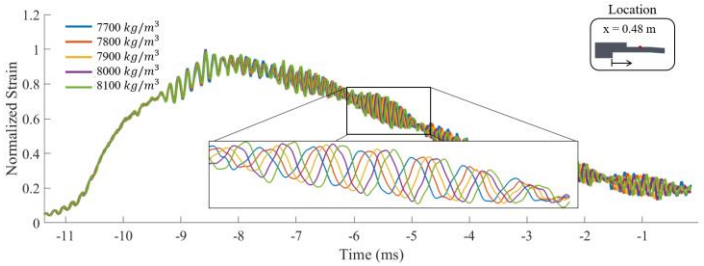

Figure 18:Normalized Tangential Strain Results for Changing Density

Table 3: Design Parameters Effect on Tangential Strain

	Range	%Δ Max. Strain	%Δ Frequency	%Δ Amplitude
Outer Radius, OR	180 – 220 mm	-42%	-6%	-81%
Elastic Modulus, E	180 – 210 GPa	-10%	+5%	~0%
Poisson's Ratio, v	0.26 – 0.30	~0%	-2%	~0%
Density, ρ	7700 – 8100 kg/m^3	~0%	-1%	~0%

6 Conclusions and Future Work

The tangential strain in a large gun barrel can be predicted using an axisymmetric model described above. The pressure gradient is approximated using Euler's Equations and anchored using experimental data at the breech (x = 0) and sidewall ($x = x_s$) . The geometry and material properties are based on a 155 mm gun barrel. The model matches well with experimental strain results at four locations near the muzzle. Here, the dominant frequency and maximum strain match within 2% at three locations, validating the ANSYS model. When each location is prescribed the maximum pressure (constant) it experiences maximum tangential strain at x = 0.48 relative to other locations. This ideal location takes into accounts the thickness of the gun barrel and maximum pressure descending along its length to achieve the location where maximum tangential strain is achieved on the sidewall.

Three different cases were run for different pressure gradients, referred to as zone 5H, 4H, and 3H which are decreasing in their respective breech pressures. The tangential

strain is seen as oscillatory in nature due to a sharp increase in pressure creating the expansion and contraction of the gun barrel. The tangential strain magnitude observed also follows the behavior of the pressure rise. Knowing these two components, the internal pressure is approximated and compared to the applied pressure in the model at the same location. A lowpass filter is applied to the results, and the linear relationship based on the theory of elasticity from Eq. 1 is used to predict the internal pressure with external strain (compensating for some error due to geometry). The predicted results for all cases are within ± 4% of the actual internal pressure. This shows promising results for a non-intrusive method for internal pressure prediction for large gun barrels.

The sensitivity study looking at geometry and material properties effect on tangential strain indicated that thickness and elastic modulus were the main contributors to changing frequency and maximum tangential strain measured. The key factors to accurately predict tangential strain are thickness of the gun barrel and the elastic modulus of the material. Poisson's Ratio and density had little to no change within the ranges simulated.

Next steps for this project are incorporating compressive stresses in the gun barrel due to the manufacturing process, incorporating parts near the breech, and providing experimental data on a small scale. Currently, the manufacturing process for large caliber guns use temperature dependent methods introducing residual compressive stresses (autofrettage) to increase the maximum allowable pressure. Additionally, another location of interest other than along the sidewall is the breech end where the maximum pressure is experienced normal to the face of the breech. Other components such as the spindle and elastomeric pad used to create a seal at the breech are not currently modeled but could be contributing factors due to different material properties and contact at this alternate location. An example of radial strain at the breech end is shown in Figure 19**.** Predicting the pressure at the breech face can be especially relevant to breech failure prevention. Although the model results indicate smaller measurable strain due to thickness at the breech and large amplitude relative to the average strain (about 2x). Finally, a smaller caliber test should be complete using a rifle or system of small scale. This will give further validation of this study using minimal resources before a full-scale test is done.

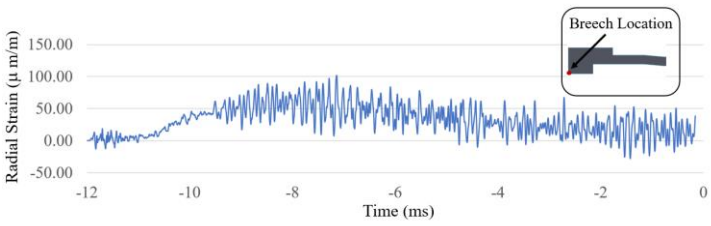

Figure 19: Strain Results at the Breech End

Acknowledgements

This material is based upon work in part supported by the U.S. Army under contract #W9124R20C0008. We particularly acknowledge Mr. Alan Tinseth, Mr. Gilbert Moreno, Mr. Gary Rosene, and Mr. Ralph Scutti for their many insights and useful discussions of this work.

References

[1] "Voluntary Industry Performance Standards for Pressure and Velocity of Rimfire Sporting Ammunition for the Use of Commercial Manufacturers," Newtown, Jun. 2018.

[2] Alen Tinseth, private communication, Nov. 2020.

[3] R. G. Budynas, J. Keith. Nisbett, and J. Edward. Shigley, *Shigley's Mechanical Engineering Design*, vol. 9. New York, NY: McGraw-Hill Companies, Inc., 2011.

[4] R. A. Leishear, "Stresses in a cylinder subjected to an internal shock," *Journal of Pressure Vessel Technology, Transactions of the ASME*, vol. 129, no. 3, pp. 372–382, Aug. 2007, doi: 10.1115/1.2748820.

[5] Albrey de Clerck, private communication, Jun. 2022.

[6] D. A. Hopkins, "Predicting Dynamic Strain Amplification by Coupling a Finite Element Structural Analysis Code with Gun Interior Ballistic Code," Aberdeen Proving Ground, MD, Oct. 1991.

[7] N. Eches, D. Cosson, Q. Lambert, and A. Langlet, "MODELING OF THE DYNAMICS OF A 40 mm GUN AND AMMUNITION SYSTEM DURING FIRING," Sep. 2009.

[8] T. D. Andrews, "Projectile driving band interactions with gun barrels," in *Journal of Pressure Vessel Technology, Transactions of the ASME*, May 2006, vol. 128, no. 2, pp. 273–278. doi: 10.1115/1.2172965.

[9] Inc. Recreational Software, "Rifle Chamber Pressure Testing Hardware & Software," 2019.

[10] R. D. Anderson and K. D. Fickie, "IBHVG2-A USER'S GUIDE," Aberdeen Proving Ground, MD, Jul. 1987.

[11] X. Dong, X. Rui, C. Li, Y. Wang, and L. Fan, "A calculation method of interior ballistic two-phase flow considering the recoil of gun barrel," *Applied Thermal Engineering*, vol. 185, Feb. 2021, doi: 10.1016/j.applthermaleng.2020.116239.

[12] P. Qu, Q. Li, and S. F. Yang, "Temperature field and thermal stress analysis of large caliber gun barrel," in *Applied Mechanics and Materials*, 2014, vol. 518, pp. 150–154. doi: 10.4028/www.scientific.net/AMM.518.150.

[13] P. Qu, Q. Li, and S. F. Yang, "Residual stress study of autofrettaged barrel under impulsive loading," in *Applied Mechanics and Materials*, 2014, vol. 518, pp. 144–149. doi: 10.4028/www.scientific.net/AMM.518.144.

[14] M. Bundy, N. Gerber, and J. Bradley, “Thermal Distortion Due to Wall Thickness Variation and Uneven Cooling in an M256 120-mm Gun Barrel,” Aberdeen Proving Ground, MD, 1993.
[15] Army, “TM 43-0001-28,” Washington, D.C., Aug. 2001.
[16] D. K. Kankane and S. N. Ranade, “Computation of In-bore Velocity-time and Travel-time profiles from Breech Pressure Measurements,” 2003.
[17] “Field Artillery Manual Cannon Gunnery Field Artillery Manual Cannon Gunnery Contents,” 2016. [Online]. Available: http://www.apd.army.mil/AdminPubs/new_subscribe.asp
[18] W. Zepp and R. Cirincione, “AD AD-E403 025 MODULAR ARTILLERY CHARGE SYSTEM (MACS) COMPATIBILITY WITH THE 155-mm M114 TOWED HOWITZER,” 2004.
[19] F. Barez, “Longitudinal Waves in Tubes Containing Stationary and Streaming Liquids,” 1978.

Appendix A Nomenclature

Table 4: Nomenclature

Symbol	Definition	Units
α	mass damping coefficient	-
β	stiffness damping coefficient	-
ε	strain	m/m
ν	Poisson's Ratio	-
ρ	density	kg/m^3
ω	angular frequency	rad/s
m	mass	kg
r	radius	m
t	time	sec
v	velocity	m/sec
x	travel coordinate, barrel reference frame	m
A	area	m^2
C	charge/propellant mass	kg
D	diameter	m
E	Elastic Modulus	Pa
IR	inner radius	m
K	stiffness matrix	N/m
L	gun barrel length	m
M	mass matrix	kg
OR	outer radius	m
P	pressure	Pa

Subscript	Definition
air	air resistance
b	breech of gun chamber
$barrel$	gun barrel
$base$	base of projectile
i	internal/inner
l	longitudinal
m	mean
o	outer
p	projectile
r	radial
res	frictional resistance
s	sidewall
so	shot out (when the projectile exits the gun barrel)
ss	shot start (when the projectile starts to move)
t	tangential

Appendix B Defining Variables in the Pressure Gradient Equation

The pressure gradient equation outlined in Eq. 6 and rewritten below points out the known values: propellant mass, pressure due to air resistance, breech pressure; as well as the unknown values: pressure due to friction, projectile mass, and projectile location. The pressure due to friction, projectile mass, and projectile location are calibrated. This calibration is detailed below.

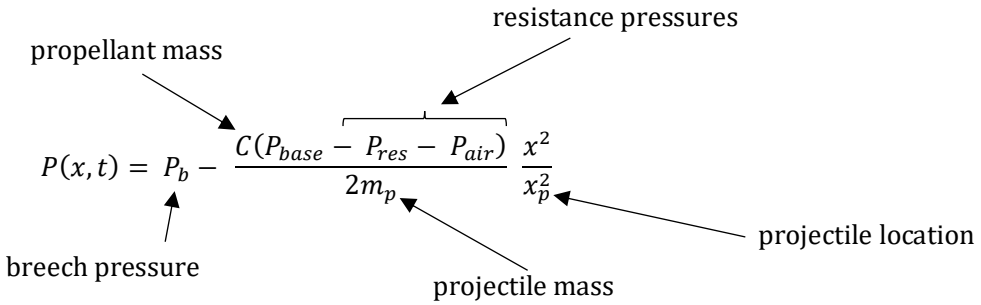

YPG has provided pressure data from a 39-cal, 155 mm barrel with Modular Artillery Charge System (MACS) propellant at zone 5H, 4H, and 3H. The breech pressure is specifically given, and propellant mass is considered constant and approximately 13 kg, 11 kg, and 8 kg respectively [15]. The projectile mass is also constant and in the feasible range of 30 kg to 40 kg [15] depending on the type.

The resistance pressures are due to air resistance and friction, thus, depending on when the projectile starts to move (shot start time). This is about when the pressure reaches 100 MPa for a large gun system [16]. The air resistance is not well documented but has been approximated as 3 MPa at maximum resistance for a 40 mm system [7]. Since this is inconsequential compared to the base pressure, it is left as 3 MPa for now. The pressure due to friction is calculated in two parts. The static friction is equivalent to the base pressure up until it reaches 100 MPa as discussed earlier [16]. Then, the kinetic friction is calibrated between zero to 100 MPa initially and has a linear trend towards zero at the shot exit time. This follows that at high speeds, the driving band around the projectile, acting as an interface to the barrel, will be worn down significantly [8]. Finally, the projectile velocity and location is estimated by integrating over the projectile acceleration discussed in the Pressure Gradient Derivation section. The shot exit time is also calculated using the projectile location. The feasible ranges are summarized in Table 5.

Computing the error between P(x_s,t) and YPG's Sidewall Pressure is estimated by three criteria. First, the maximum pressure at the sidewall must be within 5% of the experimental data. Second, the shot-out time must be within 1 ms of the experimental data. Note that the shot-out time should be zero. Thirdly, the muzzle velocity should match within 5% of the expected value for these zones. Random values are assigned to unknown variables in the feasible range, and the process goes through multiple iterations. The criteria and final solution for each case is given in Table 5 and plotted in Figure 20.

Table 5: Variables Defining the Pressure Gradient

Variable	**Assigned Value or Range**		**Final Value**	
Breech Pressure (P_b)	Pressure vs. Time Curve, Figure 14		-	
Maximum Sidewall Pressure ($P_{s,maximum}$)	5H	330 MPa (± 5%)	323 MPa	
	4H	214 MPa (± 5%)	213 MPa	
	3H	131 MPa (± 5%)	128 MPa	
Propellant Mass (C)	5H	13.27 kg	-	
	4H	10.61 kg		
	3H	7.96 kg		
Projectile Mass (m_p)	30 kg $\leq m_p \leq$ 40 kg		37 kg	
Pressure due to Air Resistance (P_{air})	3 MPa, $t_{ss} \leq t \leq t_{so}$		-	
Shot out time (t_{so})	0 ms (± 1ms)		5H	0.86 ms
			4H	0.02 ms
			3H	1.0 ms
Initial Pressure due to Kinetic Friction ($P_{res,initial}$)	$P_{res} = \begin{cases} P_{base}, & t_{start} \leq t \leq t_{ss} \\ \frac{P_{res,initial}}{t_{so} - t_{ss}} t, & t_{ss} \leq t \leq t_{so} \end{cases}$ where 0 MPa $\leq P_{res,initial} \leq$ 100 MPa		5H	38 MPa
			4H	34 MPa
			3H	27 MPa
Muzzle projectile velocity ($\dot{x}_p$)	$\dot{x}_p(t_{so}) = \int_{t_{ss}}^{t_{so}} \ddot{x}_p \, dt$	5H	863 m/s (± 5%) [8]	867 m/s
		4H	700 m/s (± 5%) [17]	704 m/s
		3H	547 m/s (± 5%) [18]	563 m/s
Projectile Location (x_p)	$x_p = \iint_{t_{ss}}^{t_{so}} \ddot{x}_p \, dt$		-	

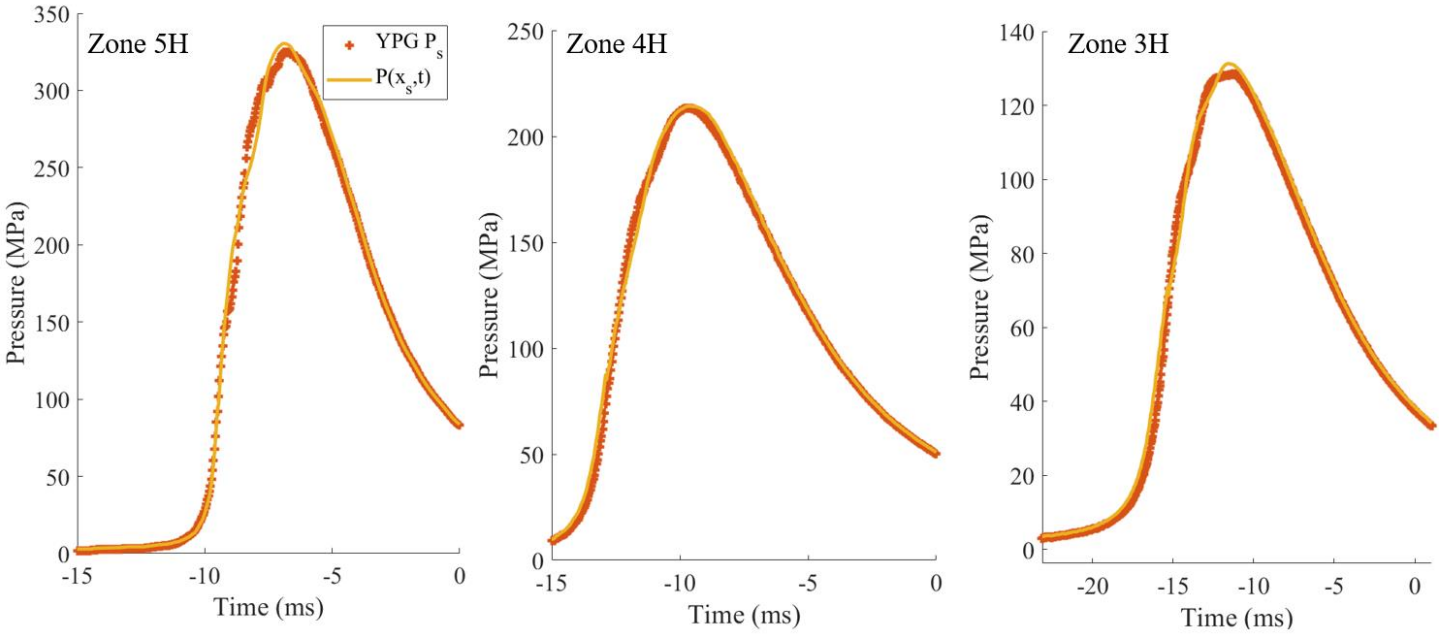

Figure 20: Matching P(x_s,t) to YPG's Sidewall Pressure

Appendix C Section Independence Study

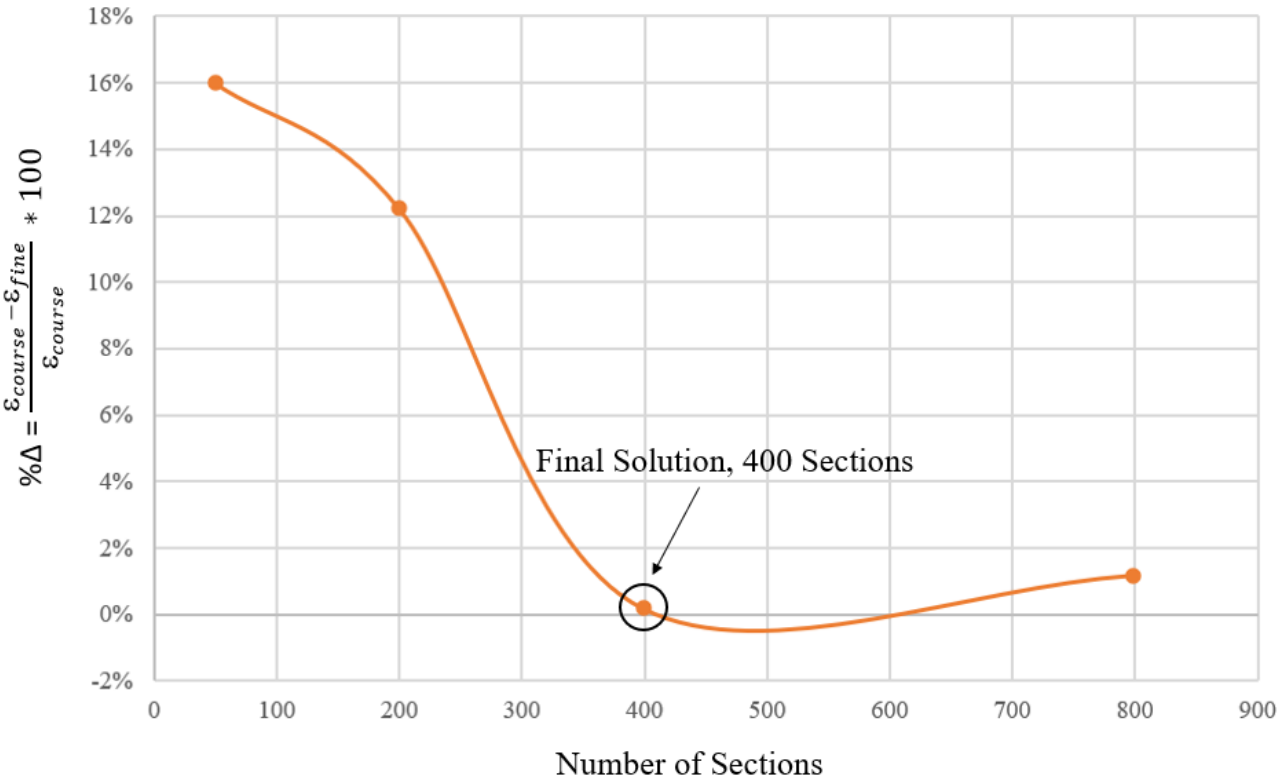

Figure 21: Section Independence Study

Appendix D Modal Analysis and Damping Coefficients

As discussed previously, the Rayleigh Damping Method estimates the damping coefficient using a linear combination of the mass and stiffness matrix, written in Eq. 7. The damping ratio plotted in Figure 22 shows the general behavior (concave in nature).

$$[C] = \alpha[M] + \beta[K] \qquad (7)$$

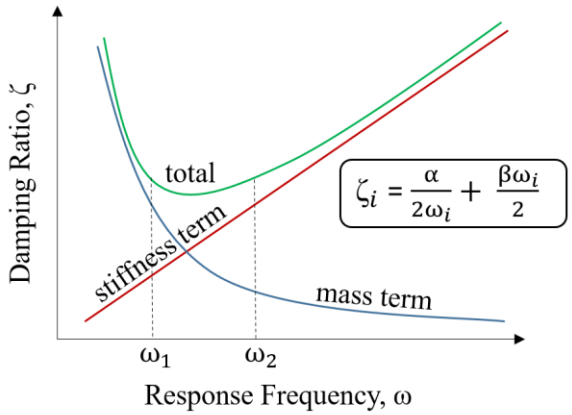

Figure 22: Damping Coefficient is a Function of Frequency

The frequency response of the gun barrel is explored using modal analysis. Figure 23 provides examples from the first ten modes extracted. The results predict many modes at different axial wavelengths and radial expansion and contraction of the gun barrel. The frequency will infinitely increase as the wavelength becomes smaller with each mode. Therefore, to determine the dominant frequencies, the initial response of the gun barrel is analyzed without damping for a step increase in internal pressure. The time increment in the transient structural simulation allows frequencies up to 125 kHz (time set to 250 kHz). Displacement is taken at different locations along the gun barrel, and dominant frequencies were extracted. This indicates near the breech; the dominant frequency is about 5.5 kHz while increasing along the length to about 10 kHz seen in Figure 25. Since lower frequencies outside the designated range are commonly overdamped using the Rayleigh Damping Method, ω_1 = 31416 rad/s (5 kHz) is used while the upper bound remains ω_1 = 62832 rad/s (10 kHz). Thus, alpha and beta are calculated in Eq. 8-9 using the damping ratio 0.003. The damping ratio was calibrated from tangential strain data from a 155 mm gun barrel [8].

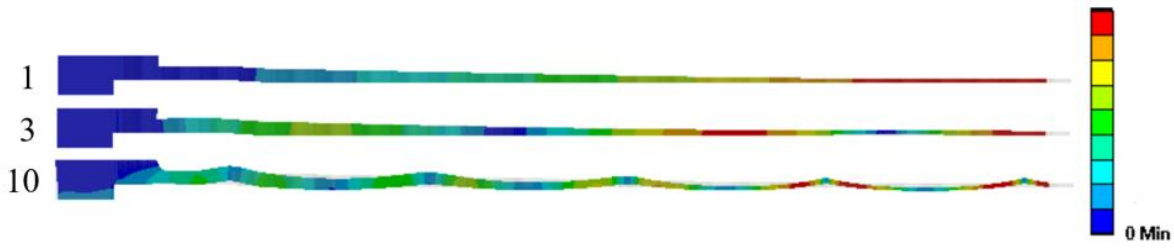

Figure 23: Modal Analysis: Modes 1,3,10

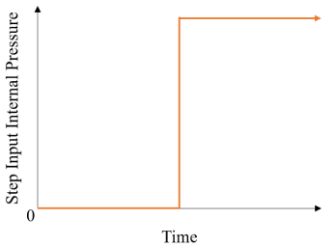

Figure 24: Step Input Applied to Internal Edges

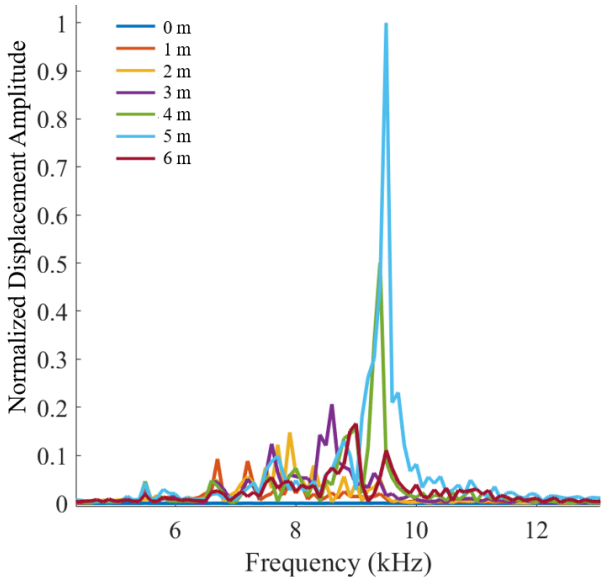

Figure 25: Frequency Response at Different Locations on the Barrel

$$\alpha = 2\zeta\frac{\omega_1\omega_2}{\omega_1+\omega_2} = 125 \quad (8)$$

$$\beta = \frac{2\zeta}{\omega_1+\omega_2} = 6.3E-8 \quad (9)$$

Appendix E Model Verification

To check the numerical model and setup, two theoretical equations are compared to numerical results for tangential strain and dominating frequency, respectively. A few assumptions were made to simplify the barrel for proper comparison. The ANSYS model does not change, but the theoretical calculations assume that the gun barrel is an infinitely long, cylinder with no end conditions so the longitudinal stress and strain is set to zero. The material properties used for calculation are highlighted in Table 2.

For the first comparison, the pressure was applied statically to all internal faces of the model and external tangential strain is predicted on the sidewall near the chamber. Then using theory of elasticity from Eq. 1, the theoretical external tangential strain is calculated and compared to the model results. The inner radius and outer radius are set to the values at the point of measurement, 93 mm and 180 mm respectively (similar to the geometry near the chamber). This comparison is made for internal static pressures from 50 MPa to 400 MPa in 50 MPa increments. The results indicate a 13.4% difference at every point in the model with reference to theoretical results seen in Figure 26. This is likely due to the infinitely long cylinder and consistent radial assumptions made since the error is consistent for the entire pressure range.

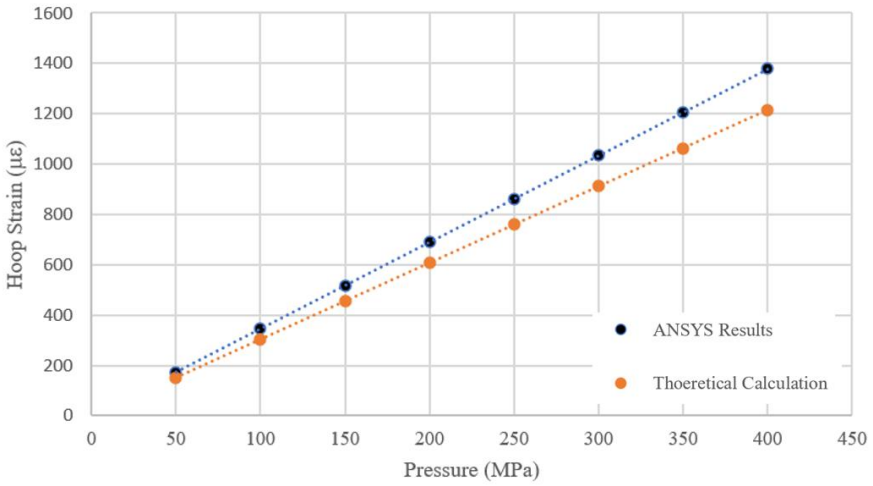

Figure 26: Model Results versus Theoretical Calculation

For the second comparison, the pressure was again applied statically to all internal faces of the model and external tangential strain is predicted on the sidewall near the chamber. A theoretical equation for the dominant or breathing frequency of the system is derived using the Rayleigh energy balance approximation seen in Eq. 10 which neglects axial dependencies [19]. This is the natural expansion and contraction of the cross section of a cylinder. The theoretical breathing frequency is calculated and compared to the model results. The mean radius in Eq. 10 is approximated based on the location along the gun barrel. Predicted external tangential strain is taken from the model and a FFT is run to find dominant frequencies. This comparison is made for 1 m increment along the length of the gun barrel seen in Figure 27. The maximum error along the gun barrel length is 3%.

$$\omega = \sqrt{\frac{E}{\frac{R_m^2(1-\upsilon^2)}{\rho_{barrel}}}} \qquad (10)$$

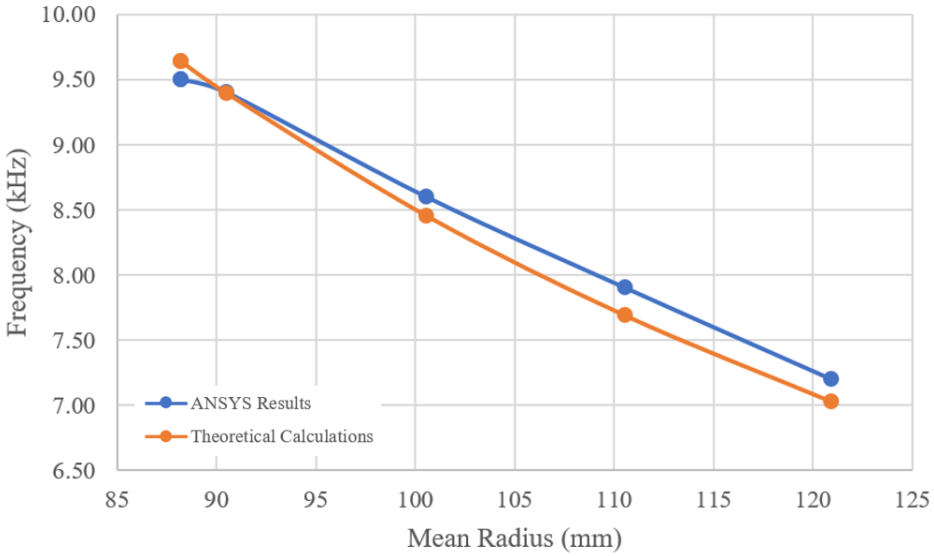

Figure 27: Model Dominant Frequency and Theoretical Breathing Frequency